
SYNOPSIS

This thesis entitled “Synthetic Studies towards the Bioactive Natural Macrolides (*Sorangicin A*, *Aspergillide B*, *Amphidinolactone A*, *Mycolactone Core*) and Novel Biocompatible Organic Nano Materials” has been divided into four chapters.

- **Chapter I:** This chapter describes development of new methodology and its application to the synthesis of bioactive complex natural products. This chapter is subdivided into three sections.
 - **Section A:** Iodine-catalyzed stereoselective synthesis of *trans*-2,6-disubstituted 3,6-dihydro-2*H*-pyran ring systems.
 - **Section B:** Application to the concise construction of C28-C37 bicyclic core of (+)-*Sorangicin A*.
 - **Section C:** Application to concise formal total synthesis of proposed structure of *Aspergillide B*.
- **Chapter II:** This chapter describes stereoselective total synthesis of *Amphidinolactone A*.
- **Chapter III:** This chapter deals with the studies towards the stereoselective synthesis of *Mycolactone* ring system.
- **Chapter IV:** This chapter describes synthesis and characterization of novel organic nano materials and their biocompatibility studies.

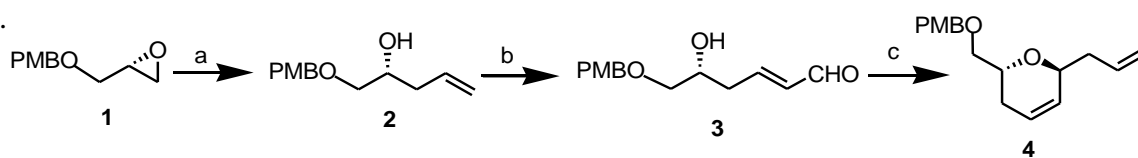
Chapter I:

Heterocyclic compounds are broadly distributed in Nature, and constitute an integral component of several polyketides, adding a significant degree of conformational rigidity in natural products and thus likely to be critical to the pharmacophore of biological activity. Among them, 2,6-disubstituted dihydropyrans, are probably one of the most common structural motifs spread across various natural products, from simple glucose to structurally complex secondary metabolites such as *lulinalide*; *leucascandrolide A*; *aspergillide A*, *B*, and *C*; *misakinolides*; *phorboxazole*; *lulimalide*; *swinholides*; *scytophycins*; and even more elaborated architectures present in *polytoxins*, *maitotoxins*, and other marine derived natural products. As a result, several approaches have been reported for the preparation of

dihydropyrans. Many of these reactions have limitations, such as the need for strictly anhydrous conditions, stoichiometric quantities of a Lewis acid initiator, or delivery of a strong Lewis acid at a low temperature. To avoid the above limitations, we have to search for a catalyst with high catalytic activity, easy availability, short reaction time, environment friendly and simple work-up procedure. Molecular iodine attracted our attention as recently it has attained considerable importance in organic synthesis because of low cost, nontoxic nature, ready availability, environment-friendly, easy handling, and high efficiency for various organic transformations to the corresponding products in excellent yields with high diastereoselectivity. Since it has been used as a mild Lewis acid catalyst for the activation of carbonyl compounds, including acetalization reactions, we envisaged that iodine could catalyze the reaction for the formation of 2,6-disubstituted-3,4-dihydropyrans starting from δ -hydroxy α,β -unsaturated aldehydes.

Chapter I, Section A:

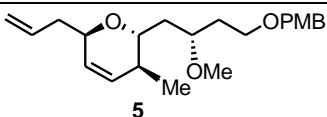
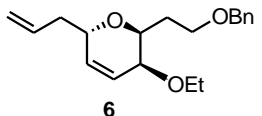
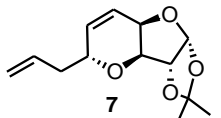
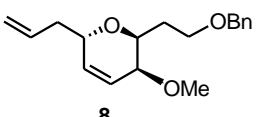
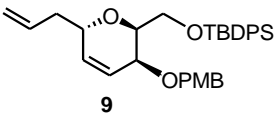
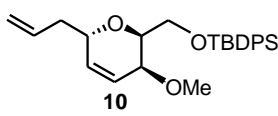
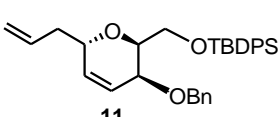
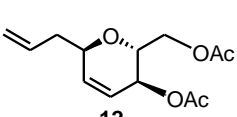
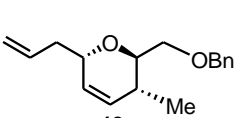
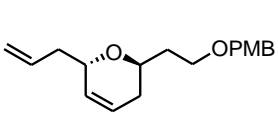
We report our research on the use of iodine as a catalyst for the construction of *trans*-2,6-disubstituted-3,4-dihydropyran under neutral reaction conditions starting from δ -hydroxy α,β -unsaturated aldehydes. In a model reaction, δ -hydroxy-enal **3** was treated with allyltrimethylsilane in CH_3CN using 5 mol % of iodine as a catalyst. After 12 h at room temperature, the reaction afforded the expected *trans*-2,6-disubstituted-3,4-dihydropyran **4** in 42% yield



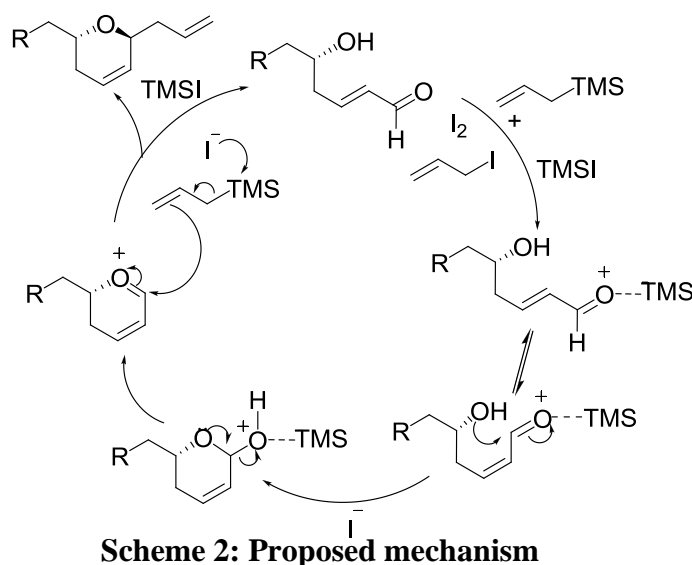
Scheme 1: Reagents and conditions: (a) vinyl magnesium bromide, CuI , $-20\text{ }^\circ\text{C}$, 88%; (b) Hoveyda-Grubbs catalyst, rt, 85%; (c) allyltrimethylsilane, I_2 , 45 min, 90%.

The stereochemistry of the product was confirmed by through investigation of spectral data. To optimize the reaction conditions, screening was performed on several parameters, such as solvents, temperature, and catalyst concentration. THF was found to be superior to other solvents. The use of 10 mol% molecular iodine (based on δ -hydroxy α,β -unsaturated aldehyde) gave the best result with a yield of 91% after 30 min of reaction.

Table 1. Iodine-catalyzed synthesis of *trans*-2,6-disubstituted-3,4-dihydropyrans

S. No.	Product ^[a]	Solvent	Time (min)	Yield ^[b]
1		THF	45	96
2		THF	30	88
3		THF	60	94
4		THF	30	93
5		THF	45	84
6		THF	40	91
7		THF	45	90
8		THF	30	87
9		THF	45	90
10		THF	30	92

To explain the formation of the *trans*-2,6-disubstituted-3,4-dihydropyran following catalytic pathways, we postulated that the product was generated with activation of aldehyde by in-situ formation of trimethylsilyl iodide and subsequent formation of an oxonium intermediate in which the stereoelectronic and/or steric factors dictate the direction of the incoming nucleophile (**Scheme 2**). To test the viability of the proposed reaction pathways, we conceived that the reaction of a δ -hydroxy α,β -unsaturated aldehyde in presence of catalytic amount of trimethylsilyl iodide (TMSI) should generate the corresponding *trans*-2,6-disubstituted-3,4-dihydropyran. Pleasingly, when 10 mol% of TMSI was added instead of molecular iodine at room temperature, the reaction completed in 10 min, which strongly supported our proposed mechanism

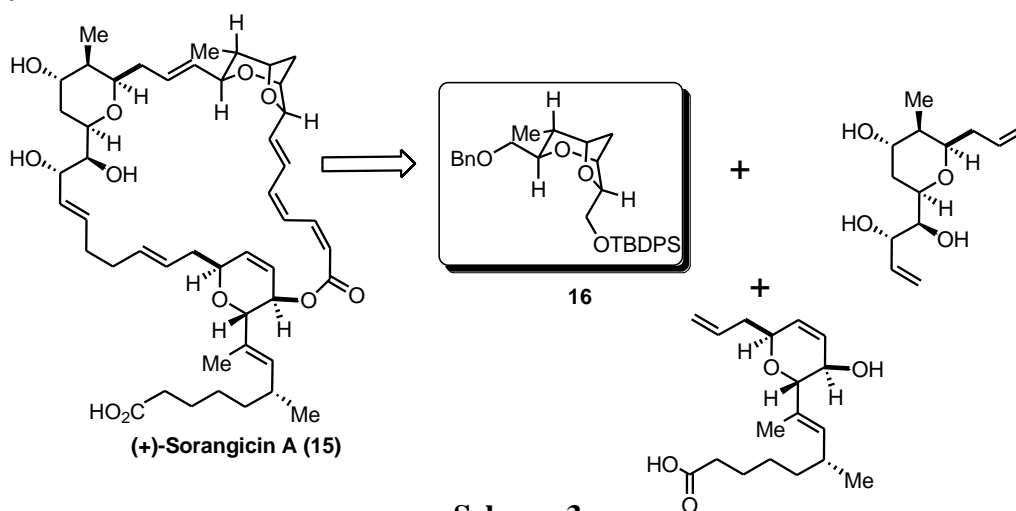


.In conclusion, we have developed a novel, practical protocol for the construction of 2,6-disubstituted-3,4-dihydropyrans starting from δ -hydroxy α,β -unsaturated aldehydes.

Chapter I, Section B:

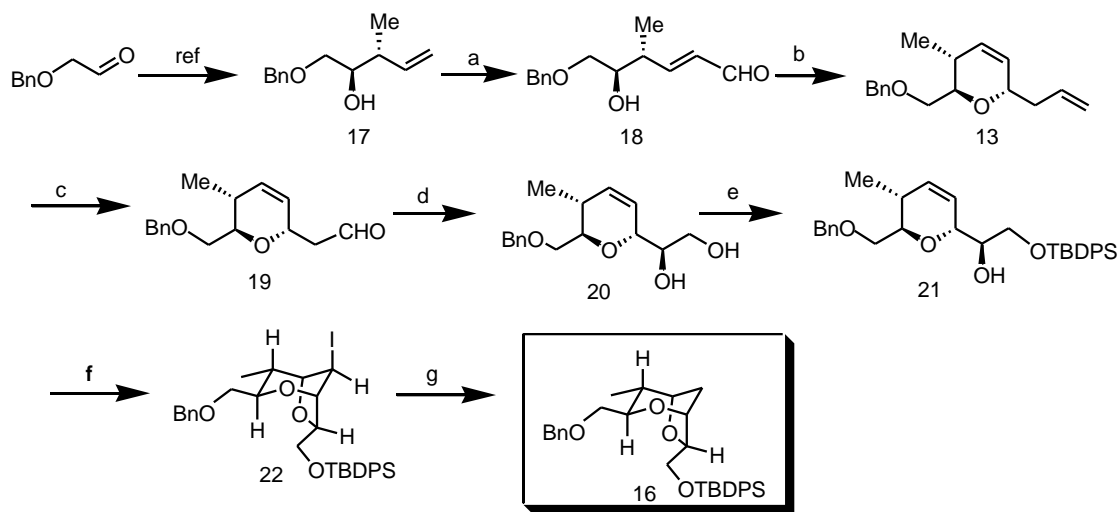
To demonstrate the applicability and generality of our method to complex biologically active natural products syntheses, we were interested in targeting the C28–C37 bicyclic ether core **16** of marine macrolactone (+)-sorangicin A (**15**).

Retrosynthesis:



We initiated the synthesis (**Scheme 3**) of **16** with a known secondary alcohol **17**, which was obtained through asymmetric crotylation of commercially available benzyloxyacetaldehyde in 96% ee under conditions originally developed by Brown and Bhat. In order to obtain the unsaturated aldehyde **18**, a cross-metathesis (CM) between **17** and acrolein (6.0 equiv) was achieved using Hoveyda-Grubbs catalyst **16a** (10 mol%) in CH_2Cl_2 at room temperature for 24 h afforded the required δ -hydroxy α,β -unsaturated aldehyde **18** in 84% yield. On treatment of **18** with 10 mol% molecular iodine in THF at room temperature gave the *trans*-2,6-disubstituted-3,4-dihydropyran **13** in 90% yield. One step conversion of terminal olefin to aldehyde **19** was achieved by modified dihydroxylation followed by oxidative cleavage of the diol in 80% yield over two steps. Direct catalytic asymmetric α -aminoxylation of the resulting aldehyde by using enantiopure proline as the catalyst and nitrosobenzene as the oxygen source and in situ reduction gave the 1,2-diol **20** in 61% yield over three steps. Selective protection of the primary hydroxyl group as its TBDPS ether yielded **20** in 92% yield. The newly created stereogenic center was confirmed by modified Mosher's method. Treatment of **21** with NIS in CH_3CN furnished the corresponding iodo ether derivative **22** as a single isomer in 81% of yield. De-iodination was achieved smoothly by treatment of **22** with Bu_3SnH and AIBN in toluene under reflux conditions to obtain **16** in 94% yield. The product was confirmed by ^1H , ^{13}C NMR and HRMS data. The stereochemistry of the

advanced intermediate was ascertained by NOE experiments.



Scheme 4: Reagents and Conditions: (a) Acrolein, Hoveyda-Grubbs catalyst, rt, 84%; (b) allyltrimethylsilane, I₂, 45 min, 90%; (c) NaIO₄, 2,6 Lutidine, OsO₄, dioxane: H₂O(3:1), 1h, 92%; (d) PhNO, D-Proline, NaBH₄, CuSO₄·5H₂O, MeOH, 12h, 61%; (e) TBDPSCl, imid, rt, 1h, 92%; (f) NIS, CH₃CN, rt, 24h, 81%; (g) AIBN, Bu₃SnH, reflux, 30min, 95%.

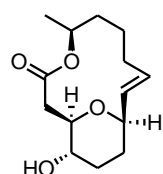
In conclusion, we have demonstrated the broad scope of the protocol to the construction of C28-C37 fragment of (+)-sorangicin A in 8 steps with 21% overall yield.

Chapter I, Section C:

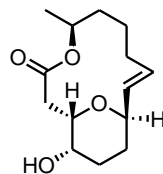
Three 14-membered macrolides, named aspergillides A, B and C, were isolated from marine-derived fungus *Aspergillus ostianus* strain 01F313, cultured in a medium composed of bromine-modified artificial seawater by T. Kusumi *et al.* in 2007. The structures of the new compounds were determined by analyses of 1D and 2D NMR spectra. Their structures were proposed to be heptaketidic 14-membered macrolides and absolute configurations were elucidated by the modified Mosher's method and chemical conversions. These three Macrolides were found to show cytotoxic activities in the micromolar range against mouse lymphocytic leukaemia cells (L1210).

We were attracted to Aspergillide B because of their unique structural motif and interesting biological activity. The major challenge from the synthetic point of view is the construction

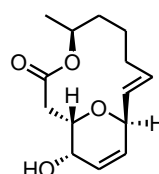
of the bridged tetrahydropyran ring with required *trans* stereochemistry.



Corrected structure of
Aspergillide A



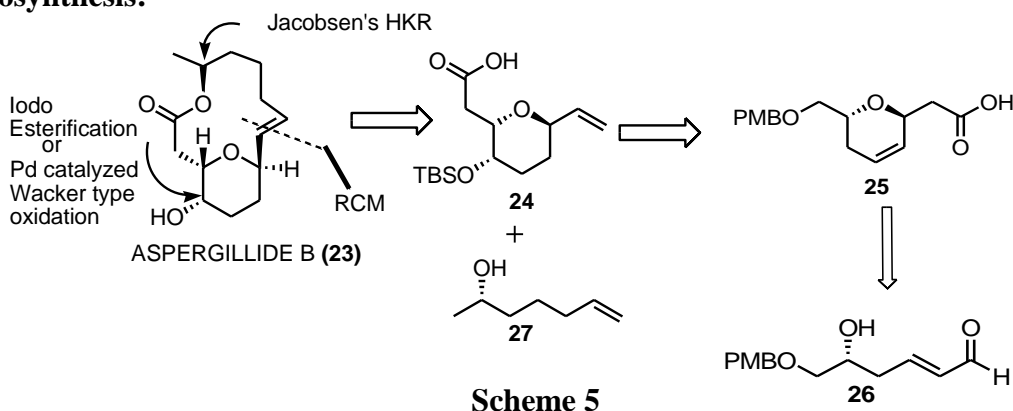
Corrected structure of
Aspergillide B



Aspergillide C

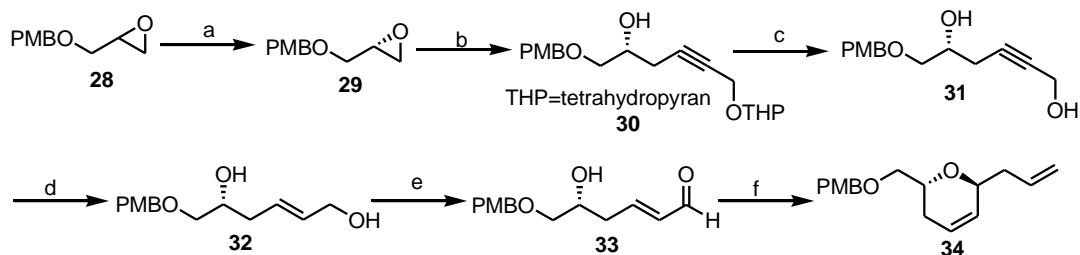
We envisioned that this goal could be achieved by our recently developed methodology and the *trans* olefin as well as the macrolactone could be achieved by a late stage RCM protocol.

Retrosynthesis:

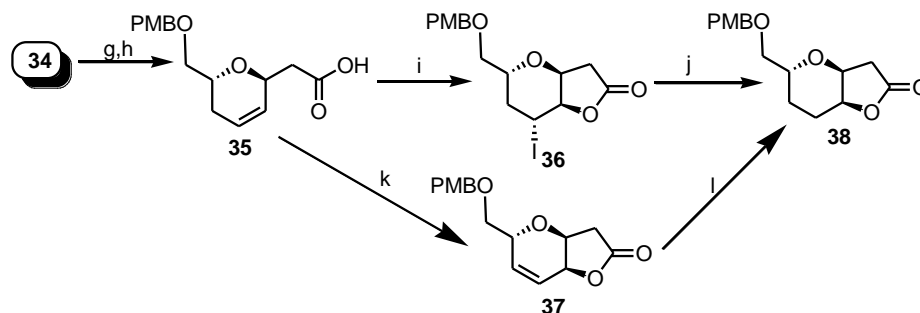


Our synthesis started (**Scheme 6**) from racemic PMB protected glycidol (**28**) which was resolved with (*S, S*) Jacobsen's Co^{III} salen to obtain **29** in 44% of yield and 98% ee. This chiral epoxide when treated with THP protected propargyl alcohol in presence of BuLi and $\text{BF}_3 \cdot \text{OEt}_2$, furnished **30** in 92% yield. The THP group was deprotected with *p*-TsOH in MeOH to produce diol **31** which was consequently reduced to *E*-olefin **32** with Red-Al in THF in 83% yield over two steps. The primary hydroxy of the diol **32** was selectively oxidized with BAIB, TEMPO to furnish **33**. With δ -hydroxy α, β -unsaturated aldehyde **33** in hand, our next target was to make the *trans*-fused pyran ring **34** which was achieved by our own developed methodology using allyltrimethylsilane as a reagent and I_2 as a catalyst in 91% yield. One step conversion (**Scheme 7**) of terminal olefin **34** to aldehyde was achieved by modified dihydroxylation followed by oxidative cleavage of the diol in 80% yield over two steps. The aldehyde was oxidized to acid **35** by Pinnick oxidation which was converted

to **38** by two different routes. First, we carried out iodo lactonization using I₂, KI in saturated



Scheme 6: Reagents and conditions: (a) (*S,S*) Jacobsen's Co^(III) salen, 12 h, rt, 44%, >98% ee; (b) *n*-BuLi, BF₃·(OEt)₂, -78 °C, 1 h, 92%; (c) *p*-TsOH, MeOH, 1 h, 95%; (d) Red-Al, rt, 12 h, 87%; (e) BAIB, TEMPO, rt, 3 h, 85%; (f) allyltrimethylsilane, I₂ (10 mol%), rt, 30 min, 91%.

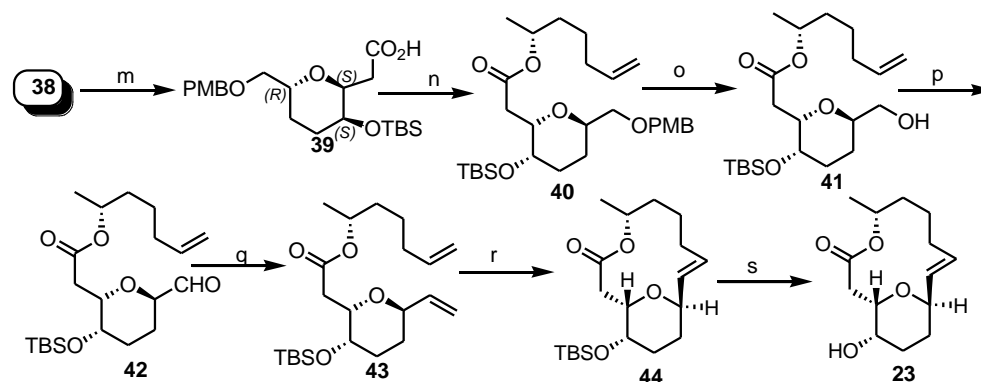


Scheme 7: Reagents and conditions: (g) NaIO₄, OsO₄, 2,6 lutidine, 3 h, 80% ; (h) NaClO₂, NaH₂PO₄, 2-methyl-2-butene; (i) I₂, KI, NaHCO₃, 6 h, 70%; (j) TBTH, AIBN, Benzene, reflux, 85%; (k) Pd(OAc)₂, Cu(OAc)₂·2H₂O, O₂, DMSO, 10 h, 95%; (l) Pd/C, H₂, 1 h, quantitative.

NaHCO₃ which produced the iodo lactone **36** in moderate yield. De-iodination was carried out using Bu₃SnH, AIBN in refluxing benzene to give the desired lactone **38** in 85% of yield. But, when we performed Pd-catalyzed Wacker type oxidation and hydrogenation protocol, we achieved **38** with 95% yield over two steps. This lactone was cleaved to its hydroxy acid (**Scheme 8**) by LiOH and then selectively protected to its TBS ether by TBSOTf, imidazole, DMAP in dry DMF to furnish **39** with 81% yield. The acid **39** was coupled with **27** under Yamaguchi condition and then PMB group was deprotected using DDQ to produce the alcohol **41** which was oxidized with Dess-Martin Periodinane and subjected to Wittig olefination to furnish the diene **43**. The diene when treated with Grubbs 2nd generation catalyst, **44** was formed as the sole product with 78% yield. Finally, TBS group was deprotected with TBAF to furnish the target molecule aspergillide B **23**.

In conclusion, we have developed a concise, stereoselective route for Aspergillide B.

Moreover, we have demonstrated the versatility of our developed methodology for natural product synthesis.



Scheme 8: *Reagents and conditions:* (m) LiOH, TBSOTf, imidazole, DMAP, 6 h, 81%; (n) 2,4,6 trichlorobenzoyl chloride, **27**, 3 h, 85%; (o) DDQ, CH₂Cl₂:H₂O/ 9:1, rt, 90%; (p) Dess-Martin Periodinane, rt; (q) PPh₃CH₂Br, *n*-BuLi; (r) G-II, CH₂Cl₂, Reflux, 3 h, 78%; (s) TBAF, THF, 0 °C, 1h, 90%.

Chapter II: Protecting Group Directed Intramolecular Nozaki-Hiyama-Kishi Reaction: A Concise and Convergent Stereoselective Total Synthesis of Amphidinolactone A

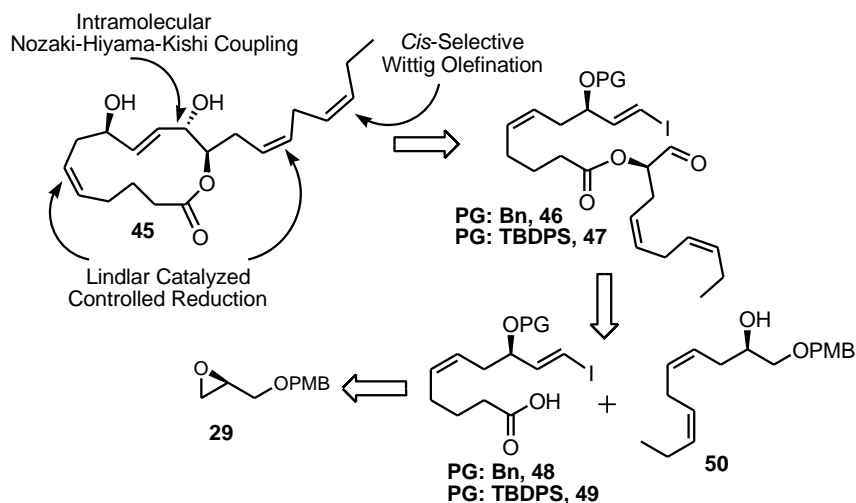
Amphidinolactone A (**45**) is a cytotoxic 13-membered macrolide, which was isolated from a symbiotic dinoflagellate *Amphidinium* sp. (Y-25) separated from an Okinawan marine acoel flatworm *Amphiscolops* sp. Their relative stereochemistry was determined by extensive NMR studies. Recently, Masahiro *et al.* reported first total synthesis amphidinolactone A and thus they confirmed that the absolute stereochemistry was identical with the proposed one (8*R*, 11*S* and 12*R*). But their approach was associated with some limitation, e.g. long reaction sequence, non stereoselective and less overall yield.

Due to its intriguing biological activity and structural complexity and to circumvent all the problems associated with the earlier synthesis, we initiated its total synthesis in a convergent manner. To achieve the asymmetric total synthesis we planned to perform stereoselective intramolecular NHK coupling reaction, Wittig olefination and Lindlar's reduction as depicted below.

Our synthesis (**Scheme 10**) started from racemic PMB protected Glycidol (**28**) which was

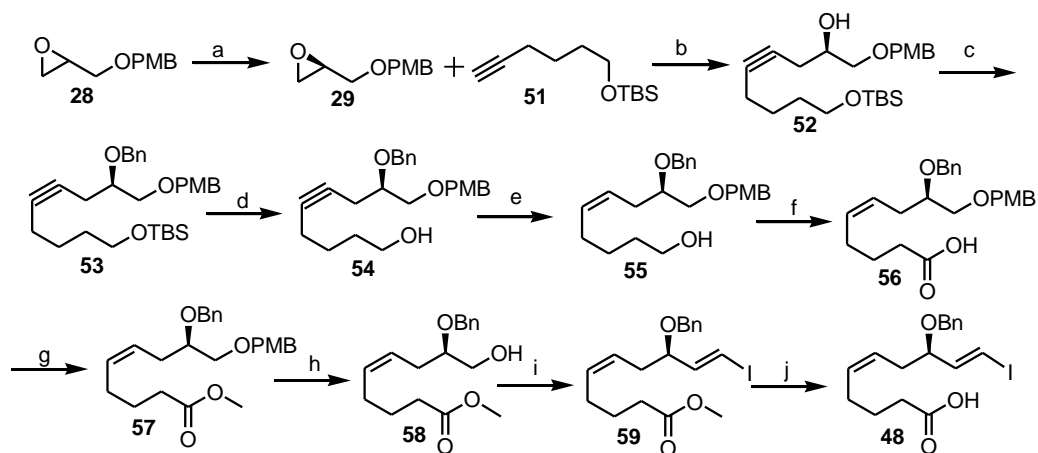
resolved with (*S,S*) Jacobsen's Co(III) salen giving **29** in 44% of yield and 98% ee. This

Retrosynthesis:



Scheme 9

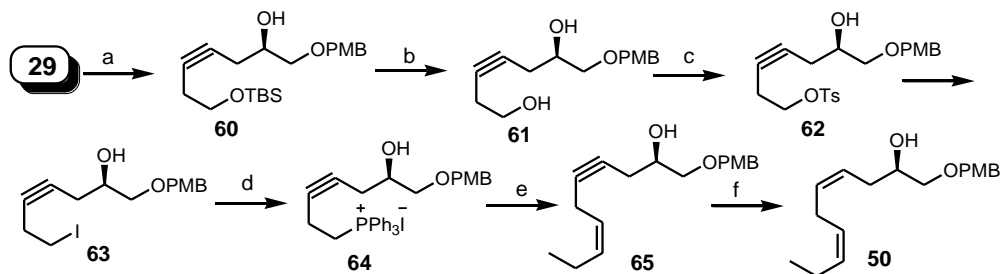
chiral epoxide when treated with **51** in presence of BuLi and $\text{BF}_3 \cdot \text{OEt}_2$, furnished **52** in 92% of yield. OBn protection, TBS deprotection with *p*-TsOH/MeOH and hydrogenation with



Scheme 10: Reagents and Conditions: (b) *n*-BuLi, $\text{BF}_3 \cdot (\text{OEt})_2$, 90%; (c) NaH, BnBr, 90%; (d) *p*-TsOH, MeOH, 91%; (e) H_2 , Pd/C on CaCO_3 , quinoline, 95%; (f) i) IBX, DMSO; ii) NaClO_2 , NaH_2PO_4 , 2-methyl 2-butene, 85% over two steps; (g) CH_2N_2 , 96%; (h) DDQ, CH_2Cl_2 : H_2O / 9:1, 89%; (i) i) DMP, 92%; ii) CrCl_2 , CHI_3 , 82%; (j) LiOH, THF: H_2O / 3:1, 91%.

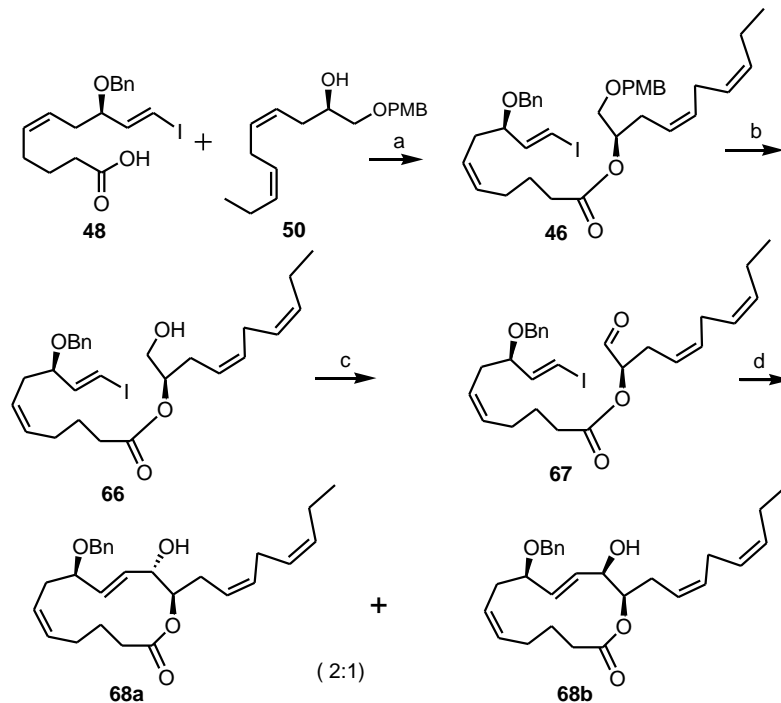
Lindlar catalyst furnished **55**, which was subsequently oxidized to acid **56** by a two step sequence. This acid was converted to its methyl ester **57** using diazomethane and then PMB group was deprotected by DDQ to give the alcohol **58**. It was converted to aldehyde by DMP which was further used for Takai olefination to give *E*-vinyl iodide **59** with good yield. Ester **59** was saponified to acid **48** using LiOH in THF/ H_2O .

To reach the second fragment, we again started (**Scheme 11**) from **29** which was treated with TBS protected homo propargyl alcohol in presence of BuLi and $\text{BF}_3 \cdot \text{OEt}_2$ to furnished **60** in 90% of yield. TBDPS group was deprotected with *p*-TsOH/MeOH and diol **61** was selectively mono tosylated with TsCl and then subsequently converted to Iodo **63** using NaI



Scheme 11: *Reagents and Conditions:* a) n-BuLi, $\text{BF}_3 \cdot (\text{OEt})_2$, 90%; b) *p*-TsOH, MeOH; c) TsCl, Et_3N ; d) NaI, acetone, reflux. e) TPP, CH_3CN , 100 °C; g) n-BuLi, Propionaldehyde; f) H_2 , Pd/C on CaCO_3 , quinoline.

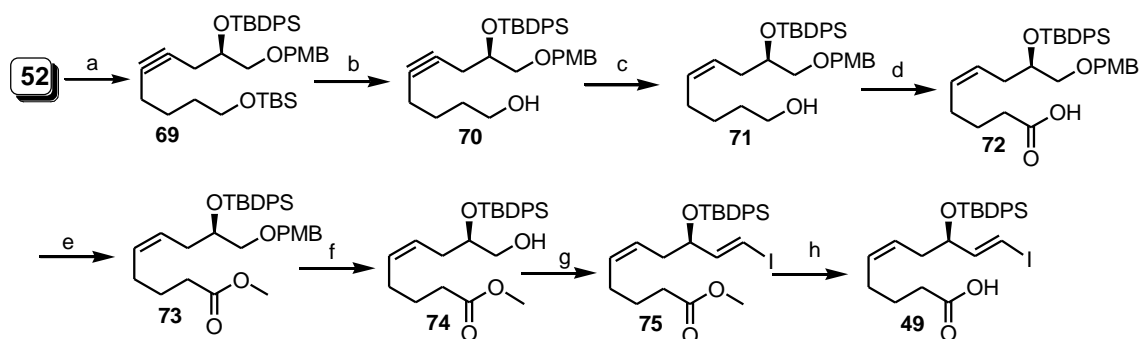
on refluxing acetone. It was converted to its TPP salt **64** for Wittig olefination. When this salt was treated with BuLi and propanal, it produced *Z*-olefin **65** as a sole product. Finally, hydrogenation with Lindlar's catalyst furnished the desired compound **50**.



Scheme 12: *Reagents and conditions:* (a) i) DCC, DMAP, CH_2Cl_2 , 0 °C-rt, 12 h, 58%; ii) EDCl, DMAP, CH_2Cl_2 , 0 °C-rt, 12 h, 70%; iii) 2,4,6-trichlorobenzoyl chloride, DMAP, THF, toluene, rt, 6 h, 89%; (b) DDQ, $\text{CH}_2\text{Cl}_2:\text{H}_2\text{O}$ /9:1, rt, 3 h, 91%; (c) DMP, CH_2Cl_2 , rt, 4 h; (d) CrCl_2 , NiCl_2 , DMSO, rt, 24 h, 81% over two steps.

With these two fragments in hand, our next task was to couple this two fragments which was achieved by 2,4,6 trichlorobenzoyl chloride under standard Yamaguchi esterification condition to produce **46** (Scheme 12). PMB group was deprotected with DDQ to give **66** which were then oxidized to their corresponding aldehydes using DMP as oxidizing agents. When, the most crucial NHK coupling was carried out in DMSO and THF (3:1) mixture, high yield was obtained although the reaction took about 24 h to completely consume the starting material. A smooth reaction ensured to afford a 2:1 mixture of inseparable diastereomeric allylic alcohols **68a/ 68b** in 84% yield.

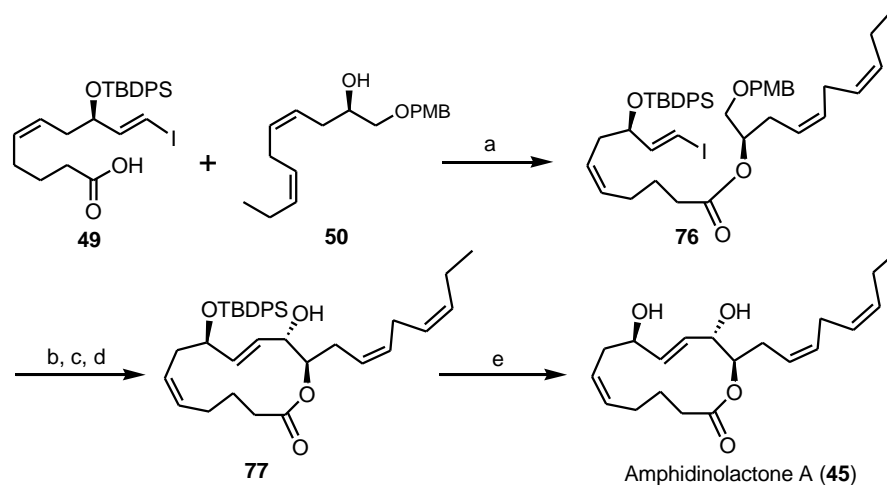
To obtain a single isomer at this juncture forced us for the judicious choice of the protecting group which can determine and influence the carbonyl facial selection. To make TBDPS protected vinyl iodide **49**, we started from **52**, which was treated with TBDPSCl, imidazole in dry DMF to give **69**. Then we carried out the same reaction sequences to reach **49** as depicted below (Scheme 13). To our surprise, TBDPS protected compound produced the desired product exclusively. Finally, TBDPS group was deprotected by TBAF to produce the final natural product **45** whose analytical data were in good agreement with the natural one.



Scheme 13: Reagents and Conditions: (a) TBDPSCl, Imidazole, DMF, 97%; (b) *p*-TsOH, MeOH, 89%; (c) H₂, Pd/C on CaCO₃, quinoline, 96%; (d) i) TEMPO, BAIB, CH₂Cl₂, rt, 3 h, 91%; ii) NaClO₂, NaH₂PO₄, 2-methyl 2-butene, 94%; (e) CH₂N₂, 95%; (f) DDQ, CH₂Cl₂:H₂O/ 9:1, 88%; (g) i) DMP, 96%; ii) CrCl₂, CHI₃, 84%; (h) LiOH, THF:H₂O/ 3:1, 90%.

In conclusion, we have accomplished the total synthesis of amphidinolactone A (**1**) in 13 longest linear steps and 22.6% overall yield from **9**. The important feature of our synthetic route is an intramolecular Nozaki-Hiyama-Kishi reaction for macrocyclization to construct 13-membered lactone and control of stereochemical outcome, after esterification between

two key intermediates prepared by concise and efficient synthetic protocol.



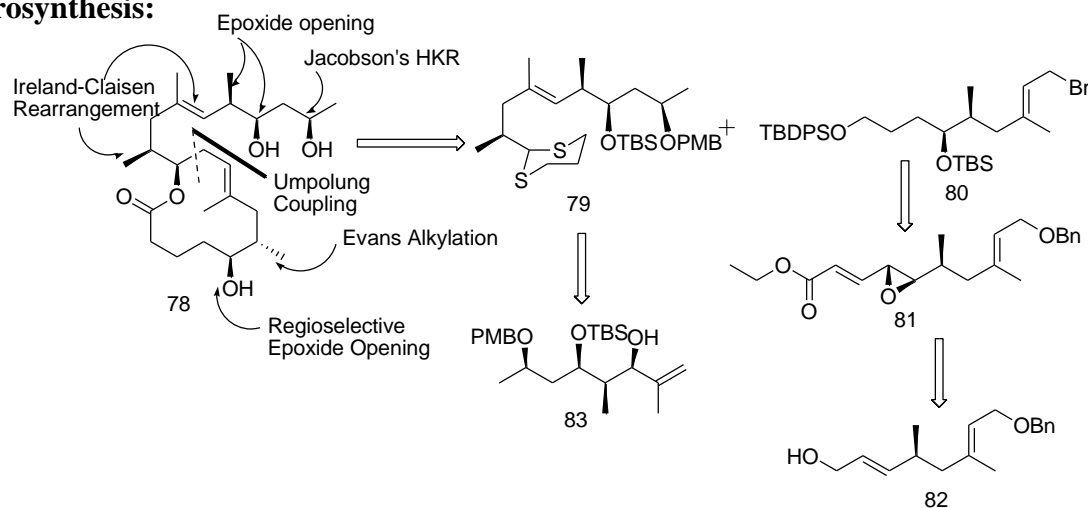
Scheme 14: Reagents and conditions: (a) 2,4,6-trichlorobenzoyl chloride, DMAP, THF, toluene, rt, 6 h, 87%; (b) DDQ, CH₂Cl₂:H₂O (9:1), rt, 3 h, 92%; (c) DMP, CH₂Cl₂, rt, 4 h; (d) CrCl₂, NiCl₂, DMSO, rt, 24 h, 85% over two steps; (e) TBAF, AcOH, THF, 0 °C-rt, 1 h, 87%.

Chapter III: Synthetic studies towards the synthesis of Mycolactone Core.

Mycobacterium ulcerans is the causative agent of Buruli ulcer, a severe human skin disease that occurs primarily in Africa and Australia. Infection with *M. ulcerans* results in persistent severe necrosis without an acute inflammatory response. Despite several attempts, no compound responsible for the cytopathic effect of this organism has been identified till 1999, when Small *et al*² identified the toxin and found it to be a polyketide. To reflect its mycobacterial source and chemical structure the toxin isolated from *Mycobacterium Ulcerans* has been named as Mycolactones A and B. Mycolactones are the first toxin isolated from *Mycobacteria* species as well as the first complex polyketide produced by a human pathogen.

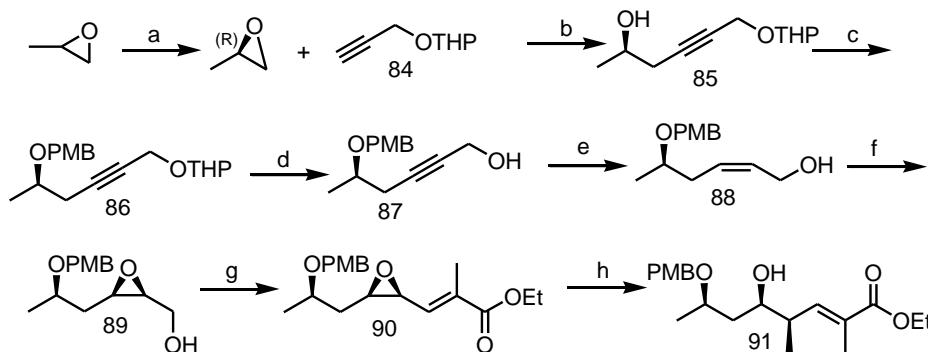
Our synthesis started from commercially available propylene oxide (**Scheme 16**) which was resolved by (*S, S*) Jacobsen's Co^(III) salen with >98% ee and 38% yield. This chiral epoxide was opened with **84** using BuLi, BF₃.OEt₂ at -78 ° C. After PMB protection and THP deprotection, the alkyne was reduced to *Z*-olefin **88** using H₂, Ni(acac)₂, NaBH₄ protocol. This *Z* allyl alcohol

Retrosynthesis:



Scheme 15

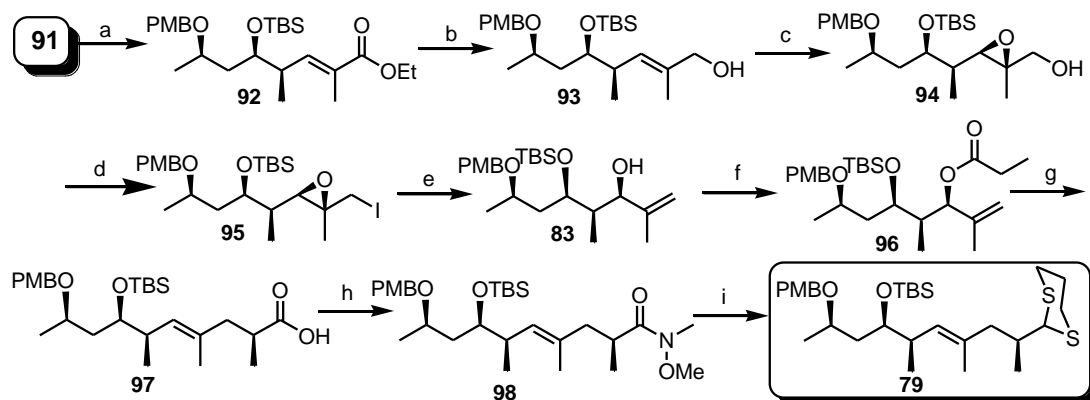
was subjected to Sharpless asymmetric epoxidation using (+) DIPT, $\text{Ti}(\text{iOPr})_4$, TBHP to get the epoxy alcohol **89** which was oxidized to aldehyde with IBX followed by Horner- Wittig-Emons olefination to produce **90** in good yield. A complete stereoselective epoxide opening was achieved by $(\text{CH}_3)_3\text{Al}$ in $\text{CH}_2\text{Cl}_2/\text{H}_2\text{O}$ to produce the secondary alcohol **91** which was protected as its TBS ether **92** by TBSOTf, Lutidine.



Scheme 16: Reagents and conditions: (a) (*S,S*) Jacobsen's Co^{III} Salen; (b) *n*-BuLi, $\text{BF}_3 \cdot (\text{OEt})_2$, 90%; (c) PMBBr, NaH, rt, 95%; (d) *p*-TsOH, MeOH, rt, 91%; (e) $\text{Ni}(\text{acac})_2$, NaBH_4 , EtOH, H_2 , rt, 98%; (f) (+) DIPT, $\text{Ti}(\text{iOPr})_4$, TBHP, -20°C , 72%; (g) i) IBX, DMSO, rt; ii) $(\text{OEt})_2\text{P}(\text{O})\text{CH}_2\text{CO}_2\text{Et}$, NaH, rt, 83%; (h) $(\text{CH}_3)_3\text{Al}$, $\text{CH}_2\text{Cl}_2\text{-H}_2\text{O}$, -40°C , 88%.

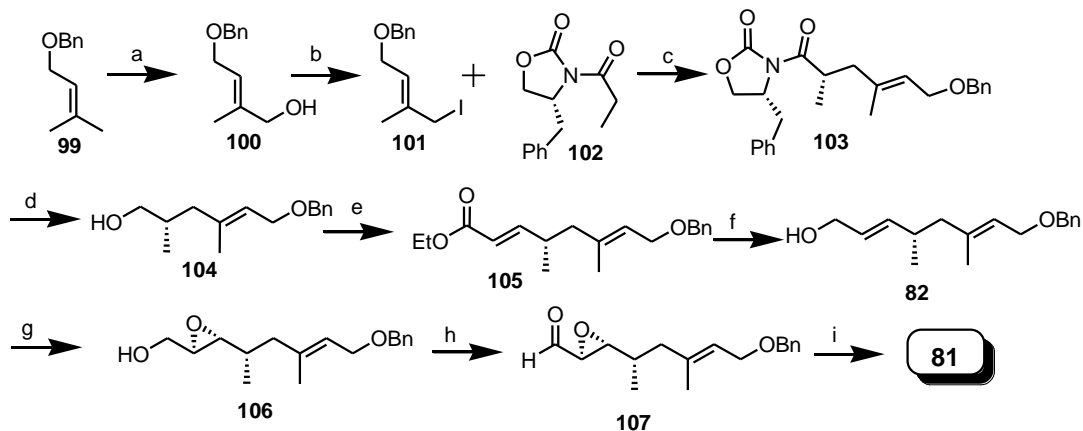
The α , β unsaturated ester **92** was reduced to ally alcohol **93** by DIBAL-H and then converted to epoxy alcohol **94** under standard Sharpless asymmetric epoxidation condition using (–) DET, $\text{Ti}(\text{iOPr})_4$, TBHP as reagents. The alcohol **94** was converted to iodo **95** which was directly treated with Zn dust/ NaI in refluxing methanol to afford allyl alcohol **83** (Scheme

17) and then, after column purification, was converted to its propionate ester **96**. Treatment



Scheme 17: Reagents and conditions: (a) TBSOTf, 2,6 Lutidine, 0 °C, 1 h, 95%; (b) DIBAL-H, 0 °C, 2 h, 91% ; (c) (-) DET, Ti(ⁱOPr)₄, TBHP, -20 °C, 3 h, 89%; (d) I₂, TPP, Imidazole; (e) Zn dust, NaI, MeOH, 6 h, 82%; (f) (CH₃CH₂O)₂O, Et₃N; (g) LDA, TMSCl, -78 °C, 3 h, 78% over two steps; (h) CH₃NH(OCH₃), EDCl, HOBT, rt, 12 h, 85%; (i) i) DIBAL-H, 1 h, -78 °C ; ii) TMSSCH₂CH₂STMS, ZnI₂, 12 h, 70% over two steps.

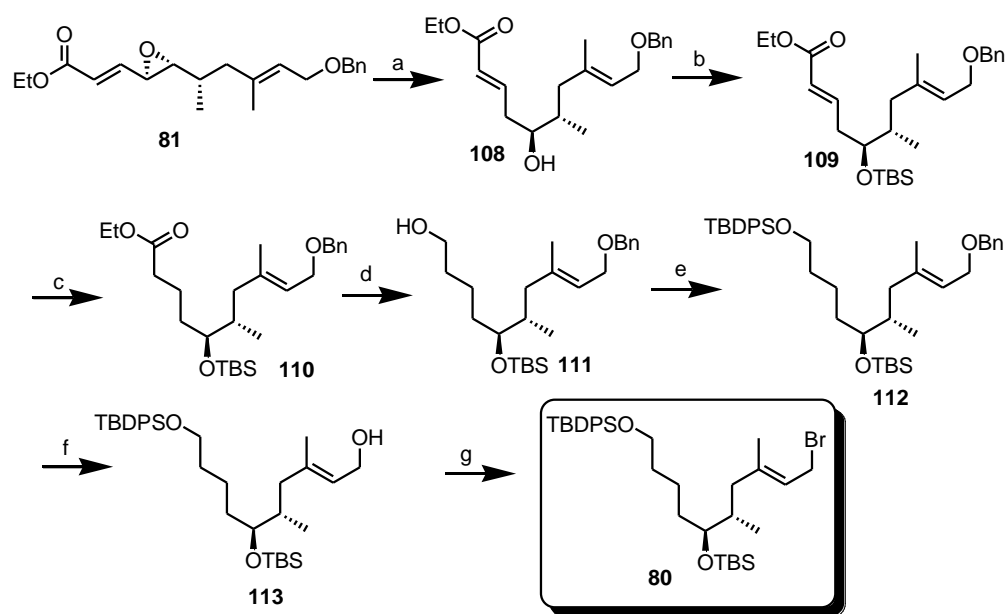
with LDA, TMSCl at -78 °C, underwent a facile Ireland-Claisen rearrangement to produce the acid **97** as a single diastereomeric product. It was converted to Weinreb amide **98** followed by treatment with DIBAL-H at -78 °C to afford aldehyde which was subsequently protected as thioketal **79** using TMSSCH₂CH₂STMS as reagent and ZnI₂ as a catalyst.



Scheme 18: Reagents and conditions: (a) SeO₂, Salicylic acid, TBHP, 24 h, 60%; (b) i) MsCl, TEA, 0 °C, 1 h; ii) NaI, acetone, 30 mins, 80% over 2 steps; (c) LiHMDS, -78 °C, 3 h, 75%; (d) LiBH₄, THF:MeOH / 4:1, 1 h, 94%; (e) i) TEMPO, BAIB, 1 h; ii) CH(PPh₃)CO₂Et, 1 h, 88% over 2 steps; (f) DIBAL-H, 1 h, 96%; (g) (-)DET, Ti(ⁱOPr)₄, TBHP, -20 °C, 8 h, 82%; (h) IBX, DMSO, 3 h, (i) (EtO)₂P(O)CH₂CO₂Et, NaH, RT, 1 h, 80%.

Our synthesis for the second fragment started from (**Scheme 18**) Benzyl protected prenyl

alcohol **99** which was oxidized with SeO_2 , TBHP to produce allyl alcohol **100** and then converted to iodo **101** by two step sequences. The iodo **101** when coupled with the auxiliary **102** under standard Evans alkylation condition furnished **103** with 72% yield with >98% de. The auxiliary was cleaved with LiBH_4 followed by oxidation and treatment with C-2 ylide to produce α,β unsaturated ester **105**. DIBAL-H reduction produced allyl alcohol **82** which was subjected to Sharpless asymmetric epoxidation with (-) DET, $\text{Ti}(\text{iOPr})_4$, TBHP to give **106**. This was converted to **81** (Scheme 19) by following two step sequence, oxidation and then HWE olefination. Next, our most crucial step was regioselective reductive epoxide opening to produce **108** which was achieved by using $\text{Pd}_2(\text{dba})_3 \cdot \text{CHCl}_3$, TPP as a catalyst and HCOOH acid as hydrogen source. This newly formed secondary hydroxy group was protected with TBSOTf to get **109** followed by selective reduction with NiCl_2 , NaBH_4 to afford its saturated ester **110**. The ester functionality was reduced to alcohol and protected as TBDPS ether to give **112**. Benzyl deprotection was achieved by Li, naphthalene which was subsequently converted to its iodo derivative **80**.



Scheme 19: Reagents and conditions: (a) $\text{Pd}_2(\text{dba})_3 \cdot \text{CHCl}_3$ (5 mol%), PPh_3 (5 mol%), HCO_2H , Et_3N , 3 h, 70%; (b) TBSOTf, 2,6 Lutidine, 0 °C, 30 min, 95%; (c) NiCl_2 , NaBH_4 , EtOH, 2 h, 90%; (d) DIBAL-H, 1 h, 96%; (e) TBDPSCl, Imidazole, 1 h, 97%; (f) Li, Naphthalene, 4h, -20 °C, 84%; (g) i) MsCl , TEA, 0 °C, 1h; ii) LiBr , Acetone, 30 min, 86% over steps.

With fragments **79** and **80** in hand, our next target was to perform Umpolung coupling

between these two. When we tried with *n*-BuLi, *t*-BuLi and *t*-BuOK-*n*-BuLi, an intractable mixture of product was obtained.

In conclusion, we have developed a stereoselective, concise route for the synthesis of the C1-C10 and C1-C19 fragment.

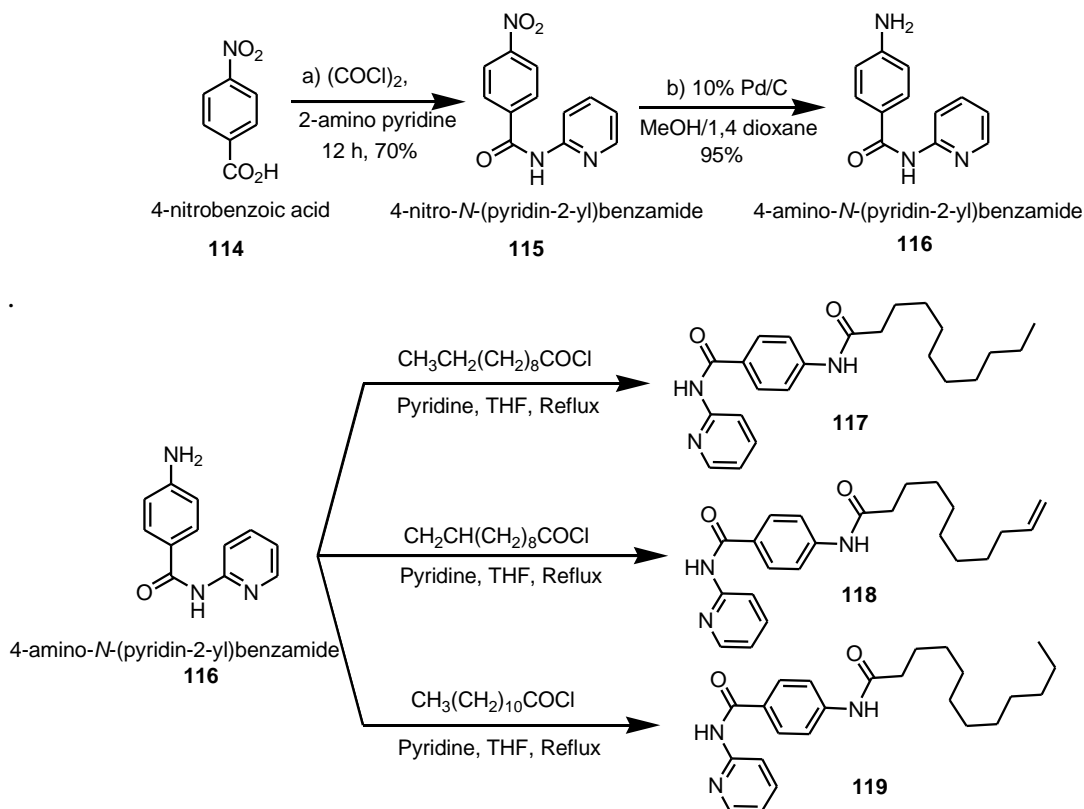
Chapter IV: Synthesis of novel organic nano materials and their biocompatibility studies.

The discoveries of buckminsterfullerene (C₆₀) and single-walled carbon nanotubes (SWNTs) represent two very significant advances in the last two decades. Both types of material have found utility in important areas such as superconductivity and molecular electronics. Whilst the synthesis and fictionalization of carbon nanotubes is now developing rapidly, the materials produced are often costly, irregular in shape, and are typically found to aggregate in large bundles, thus making manipulation somewhat less than straightforward. Given the intense focus on buckyballs and SWNTs, it is surprising that significantly less efforts have been directed to developing the synthesis of alternative multicomponent organic nanospheres and tubules.

Recently, organic tubular assemblies are of interest due to their numerous possible applications, many of which are evident from a consideration of biological systems. Inspired by the remarkable functions of tubular structures in biology, much research has focussed on the construction of simpler synthetic tubes via self-assembly. Major focus of nanomaterial development leads to bioimaging and potential use as vehicles for therapeutic delivery. Biomaterial delivery relies on three important factors: chemical modification, biocompatibility and minimal damage of the transported tissues/organs. We therefore developed nanomaterials exhibiting fluorescence either intrinsic or resulting from fluorescent molecules embedded during self-assembly that may be used as bioimaging agents both *in vivo* and *in vitro* by inhibiting rapid bleaching effect.

PABA (*p*-aminobenzoic acid) is a natural non-protein amino acid which is frequently found as a structural moiety in drugs with a wide range of therapeutic applications, such as: antibacterial, local anesthetic, anti-arrhythmic, gastrokinetic etc. So, we envisioned PABA could be the right choice as an integral component of nano materials for

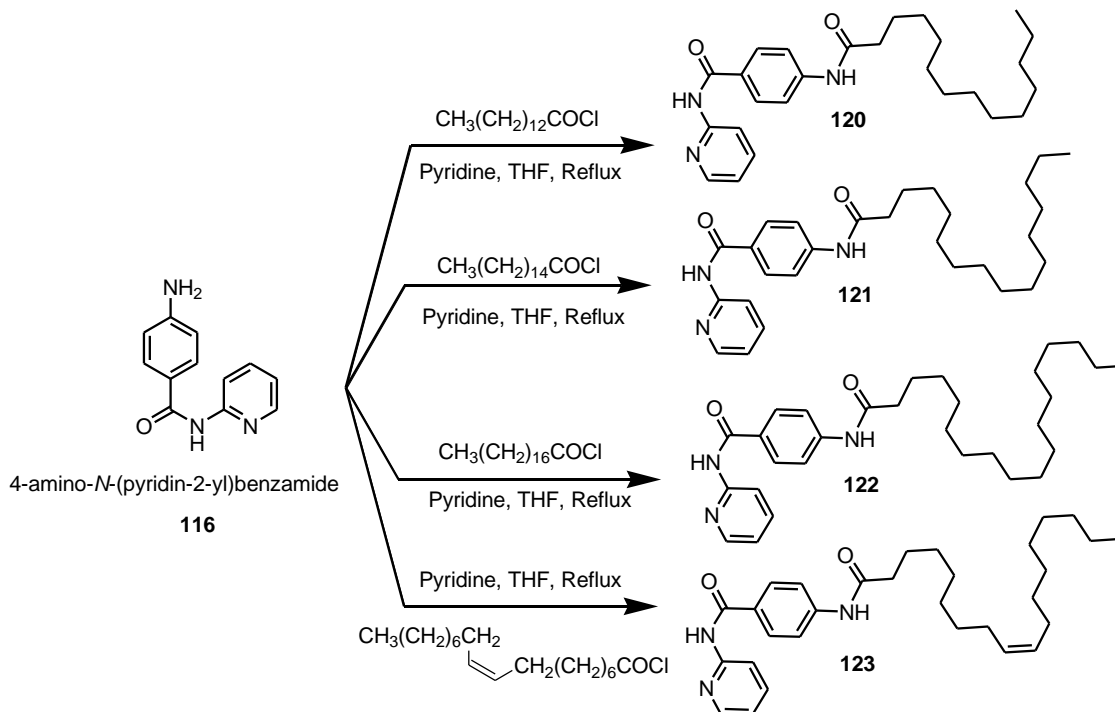
biocompatibility. Our previous studies already showed that amino pyridine moiety plays an important role for self aggregation. Herein, we report the preparation of PABA and amino pyridine based nano materials, their characterization and cell viability studies.



Scheme 21

Our chemical synthesis started from *p*-nitro benzoic acid which was converted to its acid chloride by $(\text{COCl})_2$ and then subsequently coupled with 2-amino pyridine to produce nitro benzamide. The nitro functionality was reduced to amine under hydrogen atmosphere using Pd/C as a catalyst. This amine was subsequently coupled with various acid chlorides to furnish final benzamides which were converted to different nano material of different shape and size.

Preparation and isolation of nano materials: To obtain self-assembled nanomaterials, each compound (1 mg) were added in methanol (2 mL) and heated to 60°C till it dissolved completely. Deionized water (2 mL) was added slowly at the same temperature to obtain a milky white solution which upon slow cooling to room temperature furnished cotton-like



Scheme 22

white aggregates. To prepare rhodamine B embedded fluorescent nanotube, rhodamine B solution (0.1 mL, 1 mg of rhodamine B in 5.0 mL of deionized water) was added to a preheated methanolic solution (1 mg in 2ml) prior to the addition of deionized water (2 mL) which on cooling produced pink-colored fluorescent aggregates. These aggregates were isolated under centrifuged conditions (4,500 rpm for 20 min) followed by overnight drying at 60 °C to afford 0.5 mg of final nano tubes of different shape and size.

Mechanism for self aggregation: The mechanism and the driving forces for the formation of nanometric morphologies are not clearly understood. As the two compounds possess a pyridine, benzene and alkyl chain, it is likely that hydrogen bonding, Π - Π interactions and van der Waals interactions play a major role in directing the aggregation and subsequent nanotube formation. The FT-IR study revealed two absorption bands of antisymmetric (ν_{as}) symmetric (ν_{s}) CH_2 stretching vibrational modes at 2920 cm^{-1} and 2850 cm^{-1} respectively which confirmed the presence of a highly ordered *trans* structure in the aliphatic region⁸. The absence of Amide A band attributed to free NH group (over 3430 cm^{-1}) and presence of N-H stretching frequency near 3310 cm^{-1} further indicates that all NH- groups are involved in an extensive hydrogen- bonding network. The CO

stretching band at around 1600 and 1659 cm^{-1} (amide I), and the NH bending peak near 1517 cm^{-1} (amide II) suggest β -sheets for the molecules in the solid state which are known to form weakly curved sheets. The presence of sheets, half-tubes and nanotubes give evidence for the “rolling mechanism”. The formation of the tubular structures may occur by a closure of the extended sheet along one axis of the two-dimensional layer.

Cell viability test:

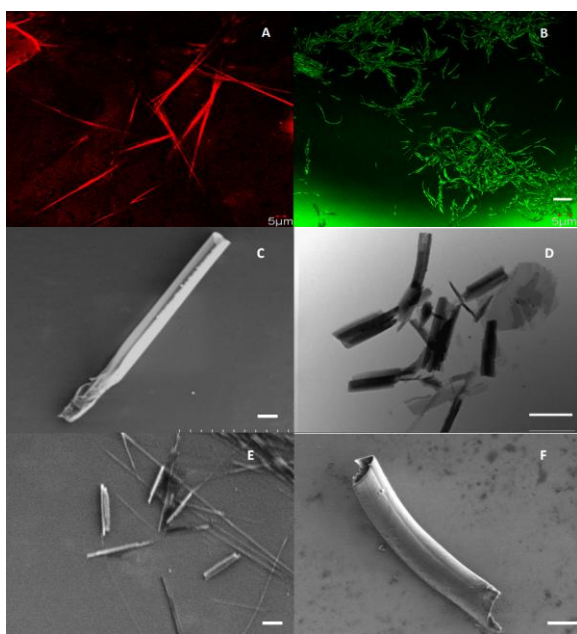


Figure 1: (A) and (B) Fluorescence Images of nanotubes **PNT-A** (from **119**) and **PNT-B** (from **112**); (Scale bar of **A** is $5\mu\text{m}$ and **B** is $10\mu\text{m}$); (C) SEM image of nanotubes from **112**; (D) TEM image of nanotubes from **112**; (E) and (F) SEM images of nanotubes from **119**; The scale bars in the panels **C,D,E** and **F** are $8\mu\text{m}$,

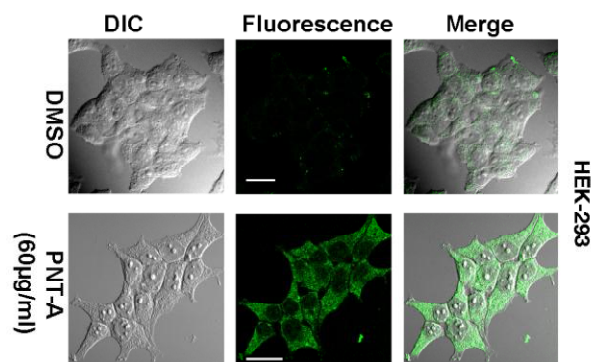


Figure 2: Cellular uptake of the **PNT-A** nanotube in human HEK-293 cells.

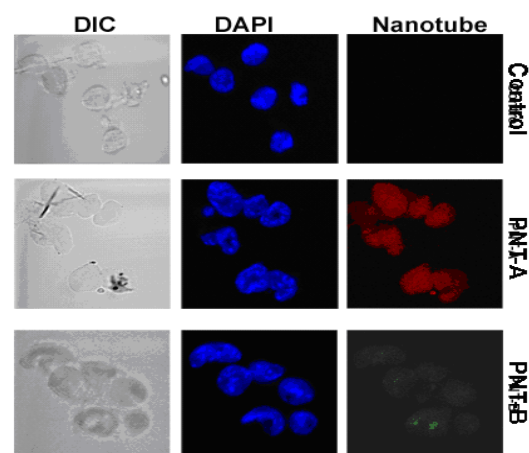


Figure 3: Uptake of two different (**PNT-A**, **PNT-B**) nanotubes in mouse embryonic stem cells $1\mu\text{m}$, $4\mu\text{m}$ and $20\mu\text{m}$ respectively.